

Photoreceptor-Specific Loss of Perifoveal Temporal Contrast Sensitivity in Retinitis Pigmentosa

Cord Huchzermeyer¹, Julien Fars¹, and Jan Kremers¹

¹ Department of Ophthalmology, University Hospital Erlangen, Erlangen, Germany

Correspondence: Cord Huchzermeyer, University Hospital Erlangen, Schwabachanlage 6, 91054 Erlangen, Germany. e-mail: huchzi@email.de

Received: February 17, 2020

Accepted: April 1, 2020

Published: May 27, 2020

Keywords: temporal vision; contrast sensitivity; photoreceptors; retinal dystrophy; retinitis pigmentosa

Citation: Huchzermeyer C, Fars J, Kremers J. Photoreceptor-specific loss of perifoveal temporal contrast sensitivity in retinitis pigmentosa. *Trans Vis Sci Tech.* 2020;9(6):27. <https://doi.org/10.1167/tvst.9.6.27>

Purpose: Inherited retinal diseases affect the L-, M-, S-cones and rods in distinct ways, which calls for new methods that enable quantification of photoreceptor-specific functions. We tested the feasibility of using the silent substitution paradigm to estimate photoreceptor-driven temporal contrast sensitivity (tCS) functions in patients with retinitis pigmentosa.

Methods: The silent substitution paradigm is based on substitution of lights of different spectral composition; this offers considerable advantage over other stimulation techniques. We used a four-primary LED stimulator to create perifoveal annular stimuli (2° inner, 12° outer diameters) and used a triple silent substitution to probe photoreceptor-selective tCS. Measurements were performed in a heterogeneous cohort of 15 patients with retinitis pigmentosa and related to those in a control group of nine color-normal healthy observers. Age differences between groups were addressed with a model of age-related normal contrast sensitivity derived from measurements in 20 healthy observers aged between 23 and 83 years.

Results: The age-related loss of tCS amounted to 0.1 dB/year in healthy subjects across all photoreceptor subtypes. In patients, tCS was decreased for every photoreceptor subtype; however, S-cone- and rod-driven sensitivities were most strongly affected. Postreceptoral mechanisms were not affected.

Conclusions: This feasibility study provides evidence that the silent substitution technique enables the estimation of photoreceptor-selective tCS functions and can serve as an accurate biomarker of photoreceptor-specific contrast sensitivity loss in patients with retinitis pigmentosa.

Translational Relevance: We aim to develop tests of visual function for clinical trials of novel therapies for inherited retinal diseases from methods that can currently be used only in vision research labs.

Introduction

Inherited retinal diseases (IRDs) impair retinal function to varying degrees. Photoreceptor loss is the predominant cause for this impairment, but it may also be a consequence of disarrangement of the photoreceptor mosaic resulting in a decrease in cone opsin density¹ and/or postreceptoral retinal remodeling.² Dysfunction of the retinal pigment epithelium may play an additional role in certain types of IRDs, for example ABCA4-, RPE65-, and MerTK-related diseases.³ In this study, we were only concerned with parafoveal and perifoveal retinal function.

The method of silent substitution (or spectral compensation) is a powerful technique using photoreceptor-isolating stimuli for investigation of retinal processing in normal subjects.^{4,5} The method implicates light substitution: light of a specified spectral composition is replaced by another light of a different spectral composition. The spectral composition and intensity of these lights are chosen in such a way that excitation, that is, the rate of photoisomerization, varies only in the target photoreceptor class, but remains constant in other classes. This property distinguishes silent substitution from selective chromatic adaptation, the method where a colored stimulus is superimposed on an adapting background resulting in

desensitizing nontarget photoreceptors while the flash specifically stimulates the target photoreceptor class (as used in short-wavelength automated perimetry).

The silent substitution method has three advantages: (1) retinal adaptation can be chosen independent of the target photoreceptor type⁴; (2) at the photoreceptor level, the contrast and, thus, the stimulus strength can be accurately quantified^{5,6}; and (3) isolation of the photoreceptor class signal is more robust than using chromatic desensitization that cannot warrant complete isolation and sometimes achieves only a bias of the sensitivity toward the photoreceptor type in question.⁷

The first two advantages of silent substitution ensure that the functions of different photoreceptor classes can be compared directly, because the photoreceptor contrast is known and their sensitivity can be measured while retinal adaptation is kept constant. Also, owing to the third advantage, rod-driven responses to silent substitution stimuli can be measured at higher (mesopic) retinal illuminances and higher temporal frequencies, thereby decreasing the necessary adaptation time. We have discussed the question whether rod-driven contrast sensitivities at high temporal frequencies might be prone to L- or M-cone intrusion previously.^{8,9} Briefly, we propose that rod-driven sensitivities at relatively high illuminances may be mediated by a faster rod pathway.

The silent substitution method was used extensively in psychophysical experiments to investigate various photoreceptor-level processing mechanisms, such as light adaptation of pathways driven by different photoreceptors,^{9,10} interactions between photoreceptor classes,^{10–14} or influence of rods on color perception under mesopic conditions.^{15,16} The silent substitution method is also used for quantifying color vision defects in the cone contrast test¹⁷ and in several computerized cone contrast tests, for example the Innova Cone Contrast Test (Innova Systems, Inc., Moorestown, NJ)¹⁸ and the Konan ColorDx CCT HD (Konan Medical USA, Inc., Irvine, CA).

Also, postreceptor signaling can be characterized using the silent substitution method. In particular, different postreceptor pathways can be probed by either varying the temporal frequency or generating stimuli that target more than one photoreceptor class either in phase or in counterphase. For example, detection of L-cone isolating stimuli is mediated by the parvocellular pathway at low temporal frequencies but by the magnocellular pathway at high temporal frequencies.¹⁹ It is also possible to generate stimuli—opponent L- versus M-cone stimuli or nonopponent L+M stimuli—that directly target postreceptor pathways.

To our knowledge, the silent substitution method has not been used to measure sensitivity changes of individual photoreceptor classes in patients with IRDs. Currently, there is a renewed interest in detailed assessment of retinal functions in patients with IRD motivated by the need to assess effects of novel gene- and stem-cell-based therapies.²⁰ IRDs affect preferentially (or exclusively) one or more of the four photoreceptor types, or their synaptic function. Sieving conjectures in Hardcastle et al.²⁰ that “each disease has unique features to understand and to address,” and that “outcome metrics must be tailored specifically for each condition” (p. 6). Frequently, selective automated perimetry, a method based on chromatic adaptation, is used to measure the functioning of affected photoreceptor classes. In particular, short-wavelength automated perimetry (using a blue stimulus on a yellow background) is used for cases of enhanced S-cone syndrome,²¹ whereas dark-adapted, rod-driven visual fields are evaluated in retinitis pigmentosa (RP).²² However, isolation of the targeted photoreceptor types can be limited in selective automated perimetry, as demonstrated recently by Simunovic et al.⁷

These findings urge that a better understanding of the changes in postreceptor signaling⁷ and of possible functional consequences of retinal remodeling² in IRDs is required. The silent substitution method has the advantages as addressed and is not affected by the concerns of the chromatic adaptation approach. It, therefore, has the potential to complement selective automated perimetry.

In our earlier studies, we measured sensitivity of all four photoreceptor classes in healthy observers. For this, we used periodic, sinusoidal stimuli.²³ These are perceived either as a flicker or as a change in hue over the exposure time. Previously, we developed a technique for measuring photoreceptor-selective contrast sensitivity using a four primary LED stimulator (developed by Pokorny et al.²⁴) and validated this approach in dichromats and a S-cone monochromat.^{8,9,25} The sensitivity to the stimuli that isolated rods and each of the three cone types was measured in normal subjects at different temporal frequencies and different mean luminances. Annular stimuli were presented perifoveally, which has the advantage of minimizing interindividual variability introduced by the macular pigment as a prereceptor filter,²⁶ and thereby avoiding extensive observer calibrations that are unpractical in a clinical setting.

The purpose of the present study was to assess the feasibility and accuracy of the silent substitution method as a psychophysical tool to quantify signal detection changes in the retinae of patients with IRD and, by this means, improve our understanding of the

involved photoreceptor types and, as well, postreceptoral mechanisms. Some authors consider techniques such as ours to be “more suited for a research environment than for a clinical trial population.”²¹ To address this concern, as a first step, we estimated perifoveal temporal contrast sensitivity (tCS), at different temporal frequencies and retinal illuminances, in a relatively heterogeneous sample of patients with RP and compared their measurements with those obtained for normal subjects. In addition, we studied age-related effects in normal subjects to be able to correct for age effects when comparing normal subjects and patients. Because photoreceptor-driven tCSs for patients with RP are currently nonexistent, we explored a possible range of changes that can be encountered. This feasibility study is necessary for future quantification of the sensitivity loss in specific RP subgroups, whose conditions will be characterized more completely, including genotype–phenotype relationships.

Methods

Subjects

Healthy control subjects ($N = 20$, 13 males; aged 23–83 years; mean age, 48.75 ± 21.22 years) were recruited among medical students of the Friedrich Alexander University, Erlangen–Nürnberg, their healthy relatives, as well as among relatives of patients of the University Eye Hospital Erlangen. All normal subjects had a best-corrected visual acuity of 0.8 or greater (Snellen charts), normal visual fields (static perimetry: G1 pattern, TOP algorithm; Octopus 900, Haag-Streit, Switzerland; mean defect (MD) < 2 dB and no three neighboring fields with a loss probability of $> 5\%$), normal IOP (Goldmann applanation tonometry), and revealed normal outcomes in a slit-lamp and funduscopic examination performed by an experienced ophthalmologist (CH). They also had normal color vision assessed using either the HCM anomaloscope (Oculus, Wetzlar, Germany) or the Farnsworth D-15 test. We also used OCT to rule out early stages of age-related macular degeneration, which can be overlooked in routine funduscopy.²⁷

Patients with a clinical diagnosis of RP were recruited from the retina clinic of the University Eye Hospital ($n = 15$; 9 males; mean age, 38.47 years; median age, 33 years; range, 21–63 years). Diagnostic criteria for RP were (1) a history of self-reported night blindness, (2) characteristic visual field defects (ring scotoma/concentric restriction with or without peripheral islands), (3) reduced or extinct International Society for Clinical Electrophysiology of Vision

standard full-field electroretinogram, and (4) typical fundus findings (attenuated vessels, retinal atrophy, bone spicules). Electroretinograms were measured with the Retiport system (Roland Consult, Germany).

Exclusion criteria for this study were unstable fixation, X-linked color vision defects, significant media opacity, cataract (including posterior subcapsular cataract), history of seizures, and the inability to understand the test requirements. Syndromic RP was not an exclusion criterion. Patients who were taking medication known to affect visual function were excluded from the analysis. One heterozygous RPGR carrier had diabetes mellitus, but no signs of diabetic retinopathy on funduscopy. Her data were included in the analysis despite the potentially negative effect on tCS,²⁸ because functional defects revealed in her outcomes in other clinical tests were clearly related to RP rather than diabetic retinopathy. No genetic testing was performed for this feasibility study, but we had a genetic classification for four patients (two with hemizygous RPGR mutations, one with a heterozygous RPGR mutation, and still another one with a USH2A mutation).

Table 1 shows the demographic characteristics of the patients (age, mode of inheritance, genotype [where available], best-corrected visual acuity, presence of cystoid macular edema, and visual field classification). We classified Goldmann visual fields according to Grover et al.²⁹

All participants gave written informed consent prior to the testing. The study adhered to the tenets of the Declaration of Helsinki and was approved by the ethics committee of the Friedrich-Alexander-University Erlangen-Nürnberg.

Instrumentation and Stimuli

Stimuli were generated using a dedicated LED stimulator that had two sets of four differently colored LEDs each (peak spectral outputs at 660, 558, 516, and 460 nm; bandwidths limited by interference filters; spectral outputs measured with spectroradiometer; Instrument Systems, Munich, Germany). Characteristics of the stimulator have been described elsewhere.²⁴ A center-surround geometry of the stimulus was produced using a Maxwellian view optical pathway.²⁴ The annulus (outer diameter of 12°) was used as the test field; the center unmodulated field (2° diameter) served as a fixation target.

An artificial pupil of 3 mm diameter was used. At the retinal illuminances that were used in our experiment, natural pupil sizes under 3 mm do not occur; hence, no dilatation of the pupil was required.²⁵ When necessary, corrective lenses were positioned right

Table 1. Clinical Characteristics of Patients With RP

Age	Sex	Eye	Dx	Genetics	LogMAR	CME	Grover	Rodb-wave ^a	Mixed a-wave ^b	Photopic 30Hz-Flicker
22	M	OD	Sporadic	—	0.097	—	IIA	0	0	0
41	F	OD	X	RPGR c.2405_2406delAG, heterozygous	0.398	—	IA	31.1	27.9	5.8
21	M	OS	AR	—	0.097	Yes	A1	0	0	0
50	M	OD	Usher II	—	0.000	—	III	0	0	0
33	M	OS	AD	—	0.097	Yes	IA	0	0	0
60	M	OD	AD	—	0.097	—	III	—	—	—
39	F	OD	Sporadic	—	0.301	—	IIB	0	0	2.4
52	F	OD	Usher II	USH2A c.2710_2720dup, homozygous	0.824	—	A1	0	0	0
25	M	OD	X	RPGR c.593G>A, hemizygous	0.097	—	A1	0	0	0
23	F	OD	AD	—	0.523	—	IA	53.1	84.6	14.2
50	M	OS	Sporadic	—	-0.097	—	III	0	21	6.0
31	F	OS	Sporadic	—	0.201	—	IIA	6.3	3.5	4.8
63	F	OS	AR	—	0.523	—	A1	0	0	0
24	M	OD	X	RPGR c.2405_2406del, hemizygous	0.301	—	III	17.9	15.9	3.0
26	M	OD	Sporadic	—	0.046	—	IIA	14.7	22.3	2.7
59	M	OD	AD	—	0.495	Yes	III	1.5	26.7	4.2

^aDark-adapted 0.01 log cd s/m².

^bDark-adapted 3.0 log cd s/m².

OD, right eye; OS, left eye; LogMAR, logarithm of the minimum angle of resolution.

behind the artificial pupil. Accurate temporal modulation of the LEDs was achieved by using a sound card (Asus Xonar D2-PM, ASUSTek, Taipei, Taiwan) to drive the LEDs.³⁰ Further details of the stimuli can be found in our previous publications.^{8,25}

The time-averaged chromaticities of the unmodulated center field and the test stimulus (surround field) were equal and close to equal energy white with coordinates of $x = 0.38$, $y = 0.28$ in the CIE-1931 chromaticity diagram. The time-averaged retinal illuminance of the surround field was 289 phot Td and of the center field 144.5 phot Td (for all stimulus conditions). The function of the dimmer steady central field was to avoid foveal stimulation through stray light.

Sinusoidal photoreceptor-isolating stimuli were calculated as described by Shapiro and Pokorny⁶ based on the Stockman and Sharpe 10° cone fundamentals^{31,32} and the scotopic spectral luminosity function.³³ A detailed table with the LED contrasts for

each photoreceptor-isolating stimulus can be found in our previous papers (Table 1 in both articles)^{8,25}; in these reports, we also provided a table showing how deviations from our assumptions about the spectral properties of the fundamentals and preretinal absorption can affect the quality of isolation and photoreceptor contrast.⁸ Briefly, under all clinically relevant conditions the encroachment of nontarget photoreceptor responses constituted maximally 5% of the contrast in the isolated target photoreceptor type. This indicates that the isolation was satisfactory for all cone- and rod-isolating conditions, as was confirmed by measurements with protanopes, deuteranopes and an S-cone monochromat.^{8,25}

Measurements were performed in the eye with better visual acuity, or in the right eye if visual acuity was equal. For adaptation, subjects remained in a dimly lit room for about 15 minutes. Prior to the experiment, subjects were informed that either luminance

or chromaticity of the test stimulus (annulus) will be temporally modulated. They were instructed to report, using a response box, whether they perceived temporal modulation of the stimulus (2AFC-yes/no-procedure). During the procedure, photoreceptor contrasts were varied by altering the modulation depth of all LEDs proportionally (i.e., without changing the ratios of LED contrasts). Thresholds were determined using a modified PEST procedure with two randomly interleaved staircases. Different conditions (isolating either individual cone types or rods) were presented in random order. As a rule, duration of the experiment was approximately 30 to 45 minutes.

For deriving a model for age-corrected normal values, initially we estimated contrast sensitivity in a sample of 20 normal subjects with an extensive age range (called the “cohort”) at a limited number of frequencies (1, 4, 10, and 20 Hz), because we wanted to avoid examination times exceeding 15 minutes. The rationale for choosing these four frequencies as was two-fold: (a) they are distributed relatively evenly over a logarithmic frequency range and (b) when L- and M-cone-isolating stimuli, and possibly also rod-isolating stimuli, are presented, the thresholds are mediated by two different postreceptoral retinal pathways—the parvocellular system at 1 and 4 Hz and the magnocellular system at 10 and 20 Hz.¹⁹ For a subsample of nine subjects (“subset”), aged 23 to 65 years, we measured contrast sensitivity at five additional frequencies (2, 6, 8, 12, and 16 Hz).

Data Analysis

For each stimulus condition, the two thresholds obtained from the interleaved staircases were averaged, and the tCS was calculated as $100/C_t$, where C_t is the corresponding Michelson cone or rod contrast (%) at threshold.

Note that the gamut of the stimulator (expressed as cone or rod contrast) is limited by the spectral distribution of the LED primaries and by the photoreceptor fundamentals, namely, 24% for L-cone isolating stimuli, 22% for M-cone isolating stimuli, 89% for S-cone isolating stimuli, and 24% for rod-isolating stimuli. When subjects were unable to see the stimuli at the maximal available contrast, the threshold was assumed to be at this maximal contrast, as a conservative estimate. To estimate the effects of one or more variables (subject group: RP vs. normal; photoreceptor type; temporal frequency) we used mixed effect models.³⁴ The subject group was treated as the fixed effect and the other variables as random effects. We used a penalized quaslikelihood technique because the data were not normally distributed.³⁵

Furthermore, we calculated MDs over a low-frequency range (MD_{low} , 1, 2, and 4 Hz) and a high-frequency range (MD_{high} , 8, 10, and 12 Hz). When subjects view L- and M-cone-isolating stimuli, and possibly also rod-isolating stimuli, these two ranges are considered to reflect flicker detection through different postreceptoral mechanisms (MD_{low} , parvocellular pathway; and MD_{high} , magnocellular pathway; as described elsewhere in this article). S-cone-isolating stimuli are hardly perceivable at the high temporal frequencies. We can reach much higher S-cone contrasts with our equipment. The MD values were expressed in dB ($1 \text{ dB} = 0.1 \log \text{CS}$) and calculated by subtracting the age-adjusted log sensitivities of patients from the normal values derived from the measurements of the full tCS functions in nine subjects. When subjects were unable to perceive the maximal possible contrast, thresholds were not taken as equal to the gamut limits, but were treated as missing values. We used *t*-tests for post hoc pairwise comparisons to explore significant deviations from 0 in differences between losses in different photoreceptor types (paired data). Holm’s method was used to correct for multiple testing (L-cones vs. rods, L-cones vs. S-cones, and rods vs. S-cones at low and high frequencies, respectively).

Results

Age Effect in Normal Subjects

For the whole cohort of healthy control subjects (aged 23–83 years), we used a linear model for the age-related change of tCS at four different frequencies (1, 4, 10 and 20 Hz). We found that for the studied age range (23–83 years), the decline of contrast sensitivity with age was relatively constant across all photoreceptor-isolating conditions (Fig. 1) with slopes close to 0.1 dB/year (equals 0.01 log CS per year or 0.1 log CS per decade) for all conditions and frequencies. We used this linear loss model in the following analysis to normalize both healthy controls’ and patients’ data by the values for the age of 40 years.

The same normalization of tCS functions was reiterated for the subset of nine normal subjects (aged 23–65 years), who undertook more extensive measurements with nine temporal frequencies (1, 2, 4, 6, 8, 10, 12, 16, and 20 Hz). Results are shown in Figure 2 and Table 2. Averaged tCS curves are shown in Supplementary Figure S1. We think that S-cone- and rod-driven contrast sensitivities at 20 Hz are not artifactual and this question is addressed in the Discussion.

The dynamic range was calculated by subtracting the instrument gamut limits from the normal values. At

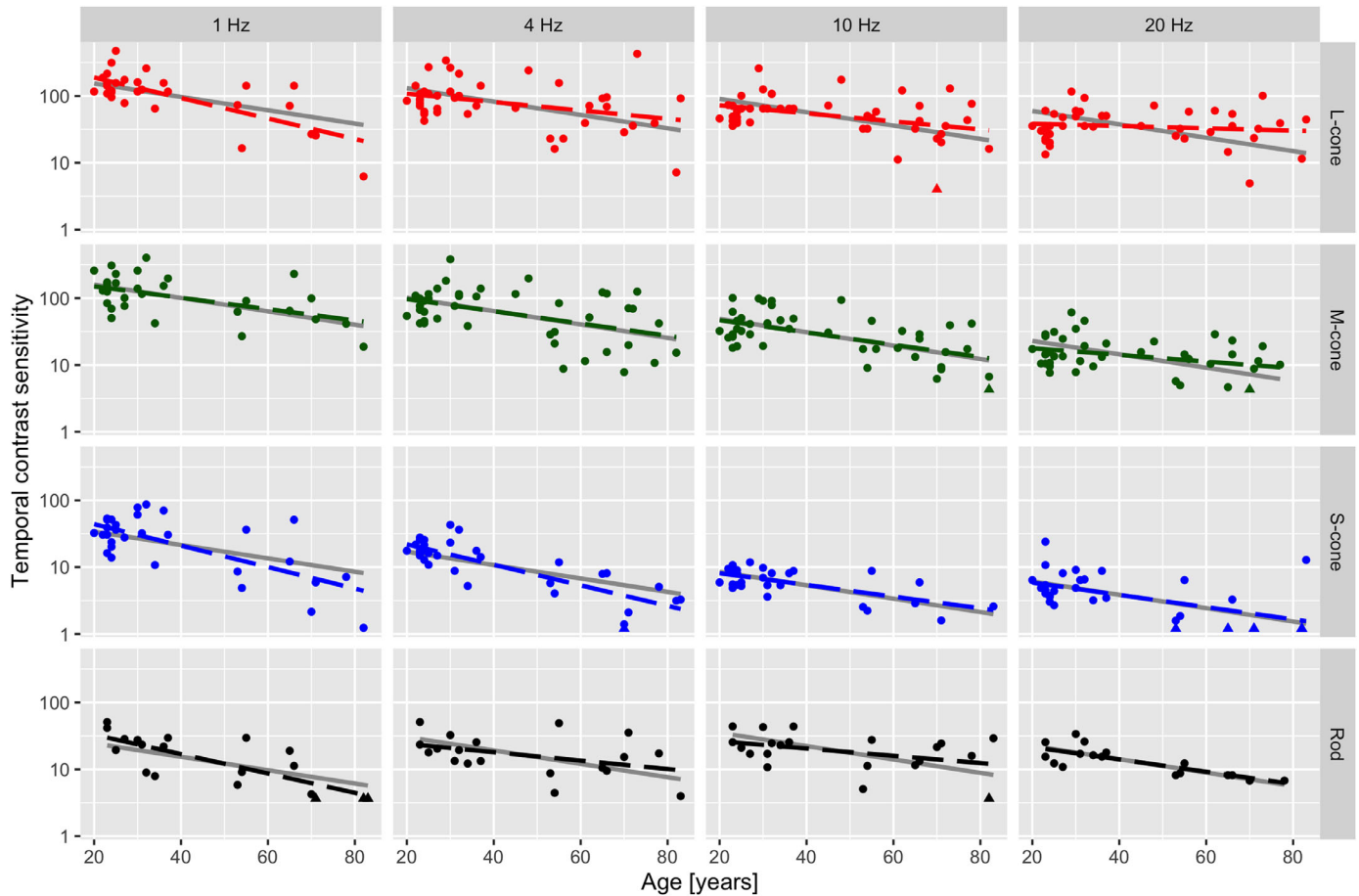


Figure 1. tCS as a function of age for four types of photoreceptor-isolating conditions. Circles show the individual contrast sensitivity values for 20 healthy control subjects; triangles indicate measurements where subjects were unable to perceive flicker at the maximal contrast (i.e., at the instrument's gamut limits). Dashed lines indicate linear regression for the given photoreceptor type and temporal frequency; solid gray lines show functions with a fixed slope of -0.1 dB/year fitted to the data by vertical shifts that seem to be a good approximation for all conditions.

the age of 40, the dynamic range is roughly between 4 and 14 dB (Table 3). Dynamic ranges for older subjects are smaller because they reveal lower temporal contrast sensitivities.

tCS Function in Patients

The age-adjusted contrast sensitivity functions for the 15 patients with RP are shown in Figure 2, too. It prompts that overall, patients with RP had lower age-adjusted sensitivities than normal subjects, as confirmed by the penalized quaslikelihood model (fixed effect value, -0.70 ; standard error, 0.18 ; $t = -4.0$; $P < 0.001$). Furthermore, it is apparent that interindividual differences are greater in patients with RP than in healthy controls subjects. Differences between measurements for the neighboring temporal frequencies are greater in patients than in the normal subjects, suggesting greater intraindividual variability,

in addition to greater interindividual variability. Notably, the L-cone- and M-cone-driven sensitivities overlap considerably, particularly at low temporal frequencies (≤ 4 Hz; Fig. 2). In some patients (even at an advanced RP stage), the tCS was in the normal range. Although, in contrast with normal subjects, patients with RP frequently did not perceive flicker at the maximum contrast (circles in Fig. 2), thresholds were measurable in most cases, implying that our measurements were not gravely limited by floor effects.

Using the obtained sensitivity measurements, we derived L-cone/M-cone and M-cone/Rod-sensitivity ratios for different temporal frequencies (Fig. 3). The following characteristics of the RP patient data can be observed. (A) Similar to normal subjects, the L/M-ratios are close to unity at low temporal frequencies (1, 2, and 4 Hz), indicating comparable sensitivities for both L- and M-cone isolating stimuli. (B) Also similar to normal subjects, the L/M ratios are

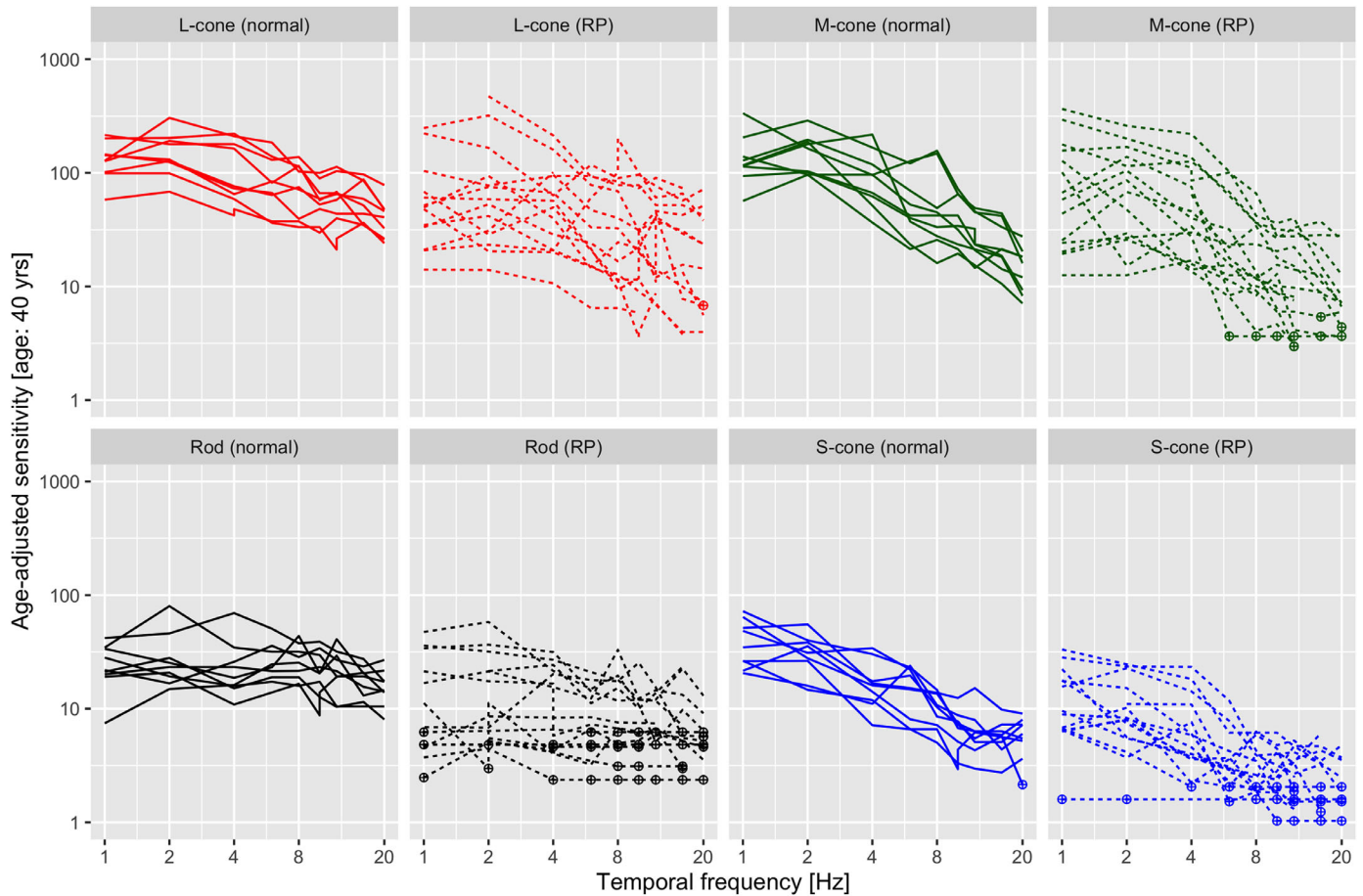


Figure 2. tCS for the four photoreceptor types as a function of temporal frequency, adjusted to the age of 40 years in normal subjects (*solid lines*) and patients with RP (*dashed lines*). Note that there are floor effects indicating that the stimulus was not perceived at the maximal Michelson contrast. For these cases (indicated by *circles*), which occurred only for the patients with RP, the threshold was set to the instrument's gamut limit as a conservative estimate. Note that the age adjustments and the distinct gamut result in different levels of the floor effects for the individual photoreceptor types.

significantly greater than 1 at higher temporal frequencies (≥ 6 Hz), implying that the subjects are more sensitive to L-cone- than to M-cone-isolating stimuli. Generally, the L-cone/M-cone ratios are similar for normal subjects and patients, suggesting that in patients with RP L-cone- and M-cone-driven sensitivities are equally affected. (C) Comparable sensitivities to M-cone- and to rod-isolating stimuli around 20 Hz, in contrast with (D) substantially larger ratios at low temporal frequencies (1, 2, 4, and 6 Hz), indicating that the sensitivity loss in rods is greater than that in M-cone cones (see Sensitivity Loss in Patients with RP: Intraindividual Comparison Between the Photoreceptor Classes). We calculated ratios for M-cone-driven:rod-driven sensitivities, because we found these ratios to be close to one at high temporal frequencies before. An analogous ratio including S-cone sensitivities was not obtained for patients with RP because often S-cone cone sensitivity could not be

determined at high temporal frequencies (see Sensitivity Loss in Patients with RP: Intraindividual Comparison Between the Photoreceptor Classes). We used the analysis of defects to statistically analyze such differences, including differences between rod- and S-cone-/M-cone-driven sensitivities.

Sensitivity Loss in Patients with RP: Intraindividual Comparison Between the Photoreceptor Classes

The dynamic ranges of the MDs are shown in Table 3 for each photoreceptor type and each temporal frequency as well as for the means at low (MD_{low}) and high (MD_{high}) temporal frequencies. The dynamic ranges are greater at low than at high temporal frequencies, and they are larger for L- and M-cones than for S-cones or rods (reflecting greater sensitivities in

Table 2. Reference Values for tCS in a 40-Year-Old Healthy Control Subject

Type	Frequency	5th Percentile	Median	95th Percentile
L-cone	1	74.5	127.8	209.7
	2	80.6	131.1	264.2
	4	44.8	74.5	216.3
	6	36.8	81.8	166.8
	8	35.0	74.8	128.8
	10	31.2	57.6	95.7
	12	23.5	61.4	108.9
	16	34.8	51.8	93.1
	20	24.8	40.7	66.0
M-cone	1	71.5	116.6	283.0
	2	96.3	164.1	252.0
	4	41.8	81.3	182.7
	6	22.2	42.2	124.7
	8	19.9	42.2	153.2
	10	20.2	34.2	69.5
	12	14.9	23.5	47.7
	16	12.0	21.1	43.2
	20	7.6	16.0	24.7
S-cone	1	21.0	34.6	68.9
	2	15.2	31.0	49.1
	4	8.7	16.0	32.6
	6	6.6	15.2	23.6
	8	5.7	10.3	14.3
	10	3.1	7.0	10.8
	12	3.5	6.2	12.3
	16	3.4	5.7	8.8
	20	2.7	6.0	8.6
Rod	1	12.1	21.9	38.9
	2	15.6	23.3	66.4
	4	12.6	18.7	55.5
	6	15.2	23.2	44.7
	8	16.1	25.4	41.3
	10	10.5	20.5	36.7
	12	10.4	21.4	37.3
	16	10.9	19.3	25.9
	20	9.0	14.5	24.8

Values are median and confidence intervals. Normal values for younger/older subjects were derived by assuming a gain/loss of 0.1 dB/year. These values were used for reporting MDs, which were calculated by subtracting the log of these values from the log tCS in the patients.

Table 3. Dynamic Ranges (dB) for a 40-Year-Old Healthy Control Subject

	1 Hz	2 Hz	4 Hz	6 Hz	8 Hz	10 Hz	12 Hz	16 Hz	20 Hz	MD _{low}	MD _{high}
L-cone	13.8	13.8	12.8	11.6	10.9	10.1	9.8	9.8	8.6	13.5	10.3
M-cone	14.0	13.2	11.4	9.7	9.4	8.5	7.1	5.6	4.3	12.8	8.4
S-cone	13.4	12.4	10.4	9.1	7.7	5.6	4.8	4.9	5.3	12.1	6.0
Rod	6.9	7.2	6.8	6.6	6.5	6.2	5.9	5.3	4.7	7.0	6.2

These values are not used for analysis, but the differences in dynamic range between conditions are important for understanding the potential value of our method, because small dynamic ranges may be an important limitation in clinical practice.

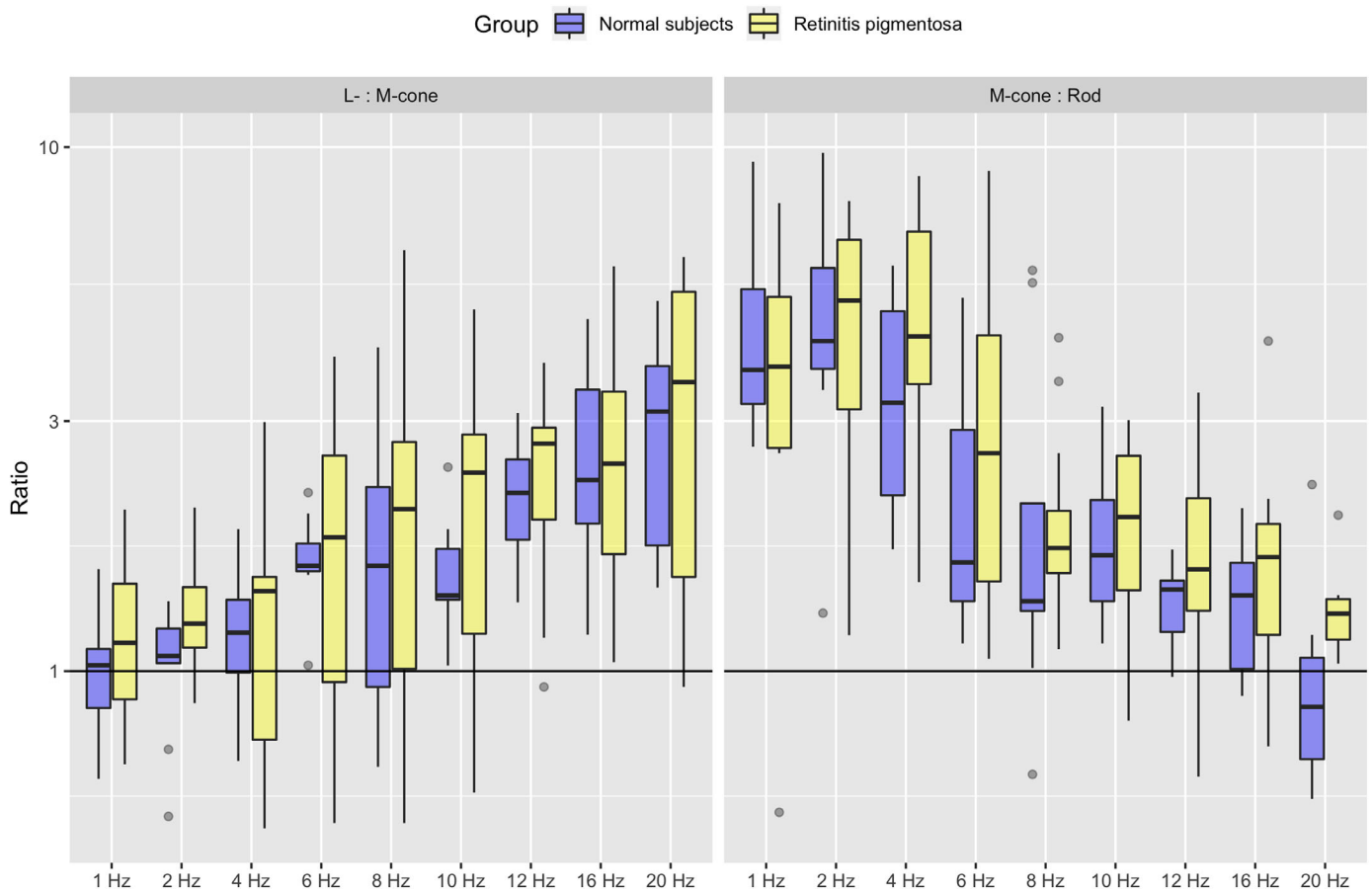


Figure 3. Ratios of L-versus M-cone-driven and M-cone versus rod-driven (R) sensitivities in normal subjects (blue bars) and patients with RP (yellow bars). There is a (nonsignificant) trend toward higher M/R ratios in patients indicating higher functional loss in rods.

normal subjects in the L-cone and M-cone isolating conditions). The S-cone-driven MD_{high} was excluded from further analyses because the dynamic range was too small.

As mentioned in the Introduction, MDs derived from application of the silent substitution method can be used to directly compare defects of photoreceptor functions in individual patients because they were obtained at identical states of adaptation. These comparisons are presented in Figure 4 for low temporal frequencies (MD_{low}) and in Figure 5 for high temporal frequencies (MD_{high}). For the RP patient group, we found that S-cone-driven MD_{low} values were higher than L-cone-driven MD_{low} values ($P = 0.046$, paired t -test; Fig. 4) and that rod-driven MD_{high} values were significantly higher than L-cone-driven values ($P = 0.023$, paired t -test; Fig. 5).

At low temporal frequencies, only L-cone- and M-cone-driven sensitivity losses were strongly correlated ($r = 0.92$; $P < 0.001$). At high temporal frequencies, in contrast, sensitivity losses were correlated between all photoreceptor subtypes ($r = 0.80$ for L-cone vs. M-

cone sensitivity; $r = 0.88$ for L-cone vs. rod; $r = 0.83$ for M-cone vs. rod; all significant at $P < 0.05$).

Discussion

The purpose of the present study was to examine the feasibility of the silent substitution method to quantify contrast sensitivity losses in the four photoreceptor types in patients with RP. Unlike measurements obtained using the chromatic adaptation approach, the present measurements were performed at identical states of adaptation for all stimulus conditions. Furthermore, temporal frequency could be varied without changing the mean state of adaptation, which enabled direct comparison of the outcomes for the individual photoreceptor types across different temporal frequencies.

For normal subjects, varying from young adults in their 20s to elderly adults in their 80s, we assessed the effect of age on contrast sensitivity and found a

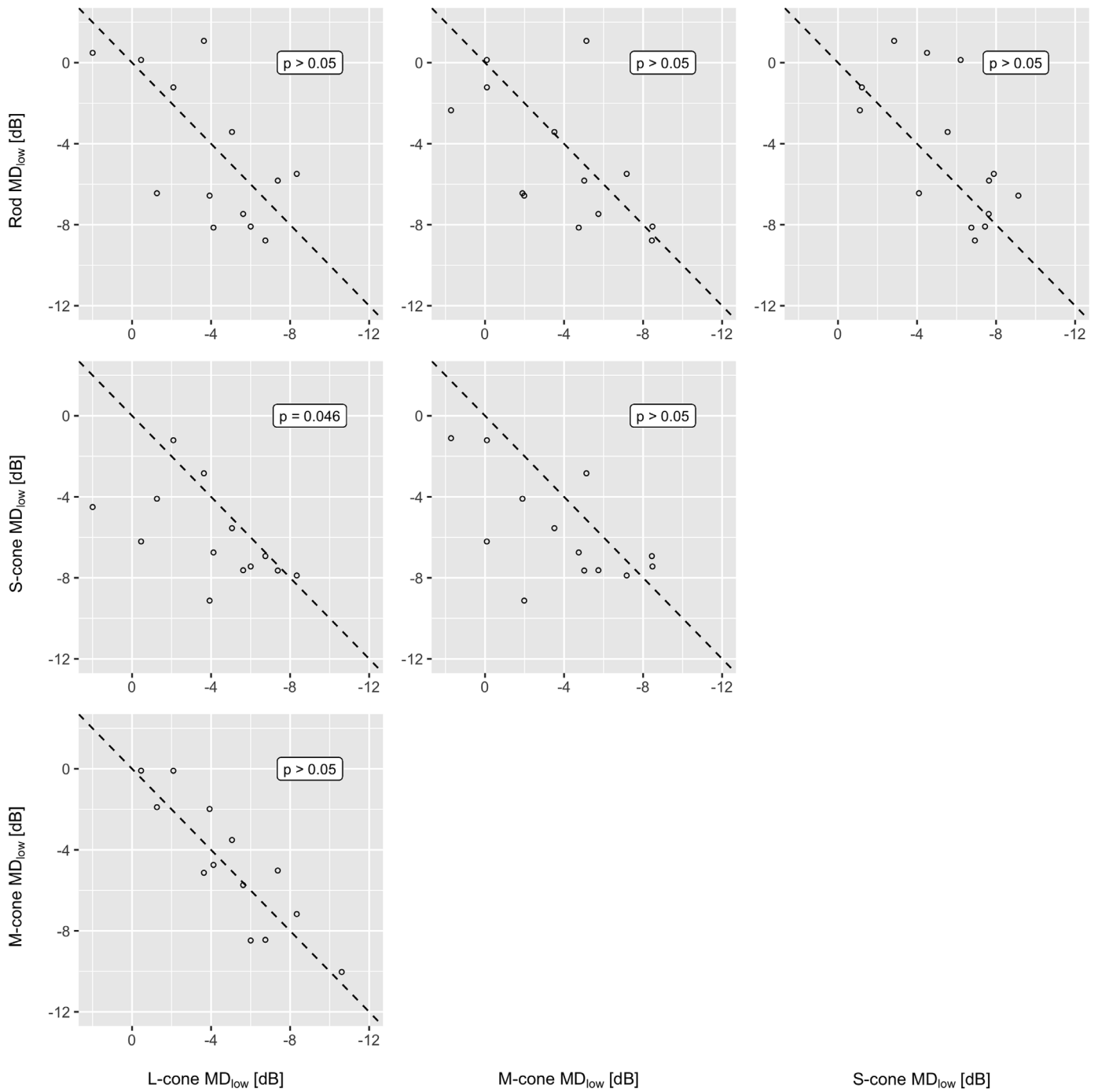


Figure 4. Patients with RP. Comparison of MD_{low} at low temporal frequencies (1, 2, and 4 Hz) between different photoreceptor types. MDs of each pair of photoreceptors are plotted against each other. Data points below the diagonals (*dashed lines*) indicate greater loss in the photoreceptor type given on the y-axis. Data points above the diagonals indicate greater loss in the photoreceptor type indicated on the x-axis. P values indicate outcomes of tests of differences in sensitivity losses in the individual photoreceptor types. Note that L- and M-cone-driven losses in sensitivity are comparable (data points are close to the diagonal), whereas S-cone losses are generally more pronounced than either L-cone, or M-cone, or rod losses. Note that a few patients with RP revealed greater rod-driven losses compared with L- and M-cone-driven losses.

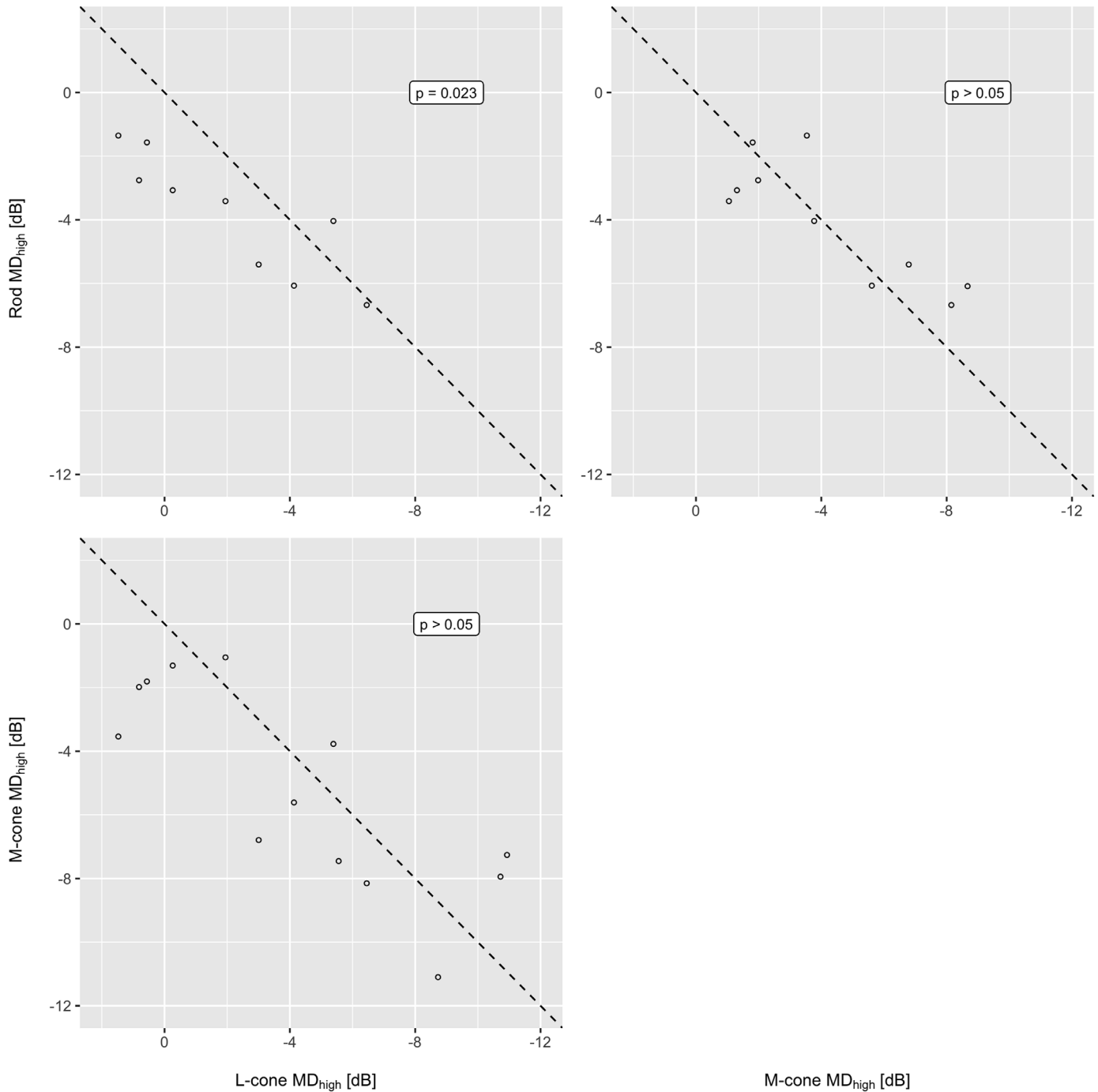


Figure 5. Patients with RP. Comparison of MD_{high} at high frequencies (8, 10, and 12 Hz) between different photoreceptor types. MDs of each pair of photoreceptors are plotted against each other. Data points below the diagonals (*dashed lines*) indicate greater loss in the photoreceptor type given on the y-axis. Data points above the diagonals indicate greater loss in the photoreceptor type indicated on the x-axis. *P* values indicate the outcomes of tests of differences in sensitivity losses in the individual photoreceptor types. Sensitivity of S-cones was omitted from this analysis since their dynamic range at high frequencies was limited. Compared with low-frequency MDs (shown in Fig. 4), sensitivity losses were more closely correlated between the three photoreceptor types.

constant age-related sensitivity loss of 0.1 dB/year for all photoreceptor types over a relatively large range of temporal frequencies (between 1 and 20 Hz). Loss of tCS over the years probably is faster in patients with

RP than in normal subjects. The additional sensitivity loss in patients with RP can be considered to be pathologic. Using an age correction for the patients' tCS based on data from normal subjects can be useful to

distinguish pathologic from merely age-related loss. Thus, it enables us to compare data of patients with those of healthy controls when there are systematic differences in the age structure.

Several previous studies, comprehensively reviewed by Werner and Steele,³⁶ demonstrated that S-cone function declines faster with age than either L- or M-cone-related functions. In contrast, Werner and Steele in their study of 76 healthy subjects aged between 10 and 84 years that estimated two-color increment thresholds of L-cone, M-cone, and S-cones³⁶ did not find this difference. A linear sensitivity decline was also found for chromatic discrimination of healthy normal trichromats in the age range between 20 and 80 or more years³⁷ by Knoblauch et al., and by other authors.^{38,39} Although experimental methods and conditions were different in the present study, our data are in close agreement with these results.

A larger cohort of normal subjects with a balanced number of subjects in each life decade would, of course, be desirable to make the model more reliable. However, for the current feasibility study the data give sufficient insights into the age effects on tCS.

Our data are in agreement with those of others who demonstrated loss of tCS to luminance flicker in patients with RP.^{40–43} Losses in cone function have also been demonstrated by tests of color vision in earlier studies.^{1,44,45} To our knowledge we, however, are the first to demonstrate the feasibility of studying contrast sensitivity loss in single photoreceptor types using the silent substitution method. Despite poor visual acuity in patients with the advanced RP, their flicker detection thresholds could be measured rather reliably. Test–retest comparisons are needed to evaluate the reliability of the measurements in greater detail.

Several mechanisms can potentially underlie the loss of tCS in RP^{41–43}: (1) a decreased number of photoreceptors; (2) a decreased number of quantum catches and isomerization in the photoreceptor outer segments; and (3) dysfunctional photoreceptors. Additional data are required to disentangle these factors.

Characteristic changes in postreceptoral signal processing reflect the way that these factors affect tCS.¹⁹ To investigate patterns of postreceptoral processing, for patients with RP and healthy controls, we compared the ratios of temporal contrast sensitivities for pairs of the photoreceptor types across a larger range of temporal frequencies (Fig. 3). At low temporal frequencies, L- and M-cone-driven temporal contrast sensitivities appeared to be similar in

patients with RP and normal subjects (L/M ratio of about unity), indicating that the detection of signal temporal modulation is mediated by the parvocellular pathway in both groups. In comparison, at high temporal frequencies, the luminance mechanism, underpinned by the magnocellular system, mediates flicker detection. We found that, in patients with RP, L-cone-driven sensitivities were about three times higher than M-cone driven sensitivities. This ratio conceivably reflects the difference in the packing densities of the L- and M-cones, with, on average, significant prevalence of L-cones.⁴⁶ The L-/M-cone ratios in patients with RP were found to be similar to those in healthy controls at all temporal frequencies. This finding suggests that postreceptoral processes in the parvo- and magnocellular pathways are either not affected by RP or affected to a similar degree. Distinguishing photoreceptoral from postreceptoral damage is not possible using psychophysical methods. Furthermore, we cannot rule out different changes in postreceptoral processing in different subgroups of our heterogenous RP population, because these analyses are carried out on averaged data.

The M-cone/rod ratios show a different dependency on temporal frequency compared with the L/M ratios. In normal subjects and patients with RP, the ratios were greater than unity at low temporal frequencies, but decreased with increasing temporal frequencies. Generally, compared with healthy controls, the ratios were higher in patients with RP, indicating that rod-driven sensitivity losses were larger than those in M-cones, confirmed by the data of individual patients (Figs. 4 and 5). The M-cone/rod ratios depended similarly on temporal frequency in patients with RP and normal subjects, again indicating that alterations in postreceptoral processing was either not present or did not alter the shapes of the tCS functions in our patients with RP. What and how postreceptoral pathways are involved remains to be determined. Cao et al.¹⁶ found that low-frequency rod-mediated color perception at mesopic illuminances is possibly based on the signal transfer from rods to cones at the gap junctions between them. Our results suggest that these gap junctions are intact in patients with RP.

At low temporal frequencies, sensitivity losses in patients with RP were greatest for S-cone-isolating stimuli compared with other photoreceptor types. Reduced S-cone-driven tCS in patients with RP were also found by Sandberg and Berson⁴⁷ and by Greenstein et al.⁴⁸ Although there is some evidence that the S-cone photoreceptors are more vulnerable,⁴⁹ the predominance of S-cone-related loss of the function is possibly caused by the scarcity of

S-cones with less redundancy and by a limited response range.⁵⁰

Functional losses at high temporal frequencies were more closely correlated between photoreceptor subtypes than at low frequencies, indicating a common mechanism of impairment for all photoreceptor types. In contrast, differences in MD between the photoreceptor types at low temporal frequencies were greater. Although this might be caused by a possibly higher retest variability at low frequencies, preliminary results suggest that this variability can possibly be explained by other clinical parameters (Huchzermeyer, et al. *IOVS*. ARVO 2020: Abstract E-Abstract 2336). Thus, tCS measurements at low frequencies may offer a better insight into pathophysiologic mechanisms of RP. However, more detailed analyses are required to substantiate this conclusion.

The key findings of the current study on tCS loss in patients with RP can be summarized as follows: First, RP results in reduced tCS in the perifovea, although in some cases tCS is relatively preserved even at advanced stages of the disease. (Note that we measured temporal function in an area that is an island of relatively preserved function in many patients.) Second, rods and S-cones are more strongly affected than L-cones and M-cones. Functional losses of different photoreceptor types are more closely correlated for temporal modulation at high temporal frequencies than at low temporal frequencies. Third, there is no indication that functional losses are related to either retinal remodeling or other changes in postreceptoral mechanisms. However, alterations in postreceptoral processing cannot be ruled using our data. We conclude that the measuring photoreceptor sensitivities by using the silent substitution method can be used to quantify sensitivity losses in RP and to draw conclusions about the retinal mechanisms that may be affected in the condition.

This study has several limitations. In particular, we examined a heterogeneous group of patients with RP, whose genetic profiling was not performed, so that a genotype–phenotype correlation could not be assessed. Also, the size of the patient population was relatively small. Nevertheless, the outcome of the present study is encouraging for future investigations with larger, more homogeneous and genetically better characterized patient groups. Although, the Farnsworth D15 has been used to rule out X-linked color vision defects in a few normal subjects and it may pass mild anomalies, we are confident that no color anomalous subjects have been included in our study, because anomalous trichromats also have different L- and

M-cone–driven tCS functions (data not published), which we did not encounter in the patients with RP.

There are a few methodologic aspects that need to be addressed in future studies that will use the present approach. First, the reproducibility of the measurements has not yet been tested, so test–retest experiments are required to assess repeatability of the measurements.

Second, our current equipment does not allow generation of spatially complex photoreceptor-isolating stimuli, such as those used, for instance, in perimetry or campimetry. Commercial monitors cannot be used because four primaries are necessary.⁶ Custom-built monitor solutions are technically feasible.

Third, the silent substitution method has not been implemented in perimeters. This is because, when light is added at the probed location, the intensity of other wavelengths would have to be decreased at the same location.

Fourth, we assumed identical photoreceptor fundamentals for all observers. However, interindividual differences may be inherent to variability in the measurements. In the present experimental design, we minimized the risk of incomplete photoreceptor isolation owing to individual variability in macular pigment density, by using perifoveal stimuli ablating the central two.⁵¹ A possible way to correct for individual variations caused by other factors—preretinal filtering, lens opacity, and/or spectral sensitivity of the photoreceptor opsins—is to use observer-specific calibrations by color matching or heterochromatic flicker photometry.^{15,52} However, such calibrations are time consuming, difficult to carry out for untrained subjects, and generally not feasible for patients with low vision.

Conclusions

The present study demonstrated the feasibility and accuracy of psychophysical measurement of tCS using the silent substitution method for quantifying sensitivity losses in individual photoreceptor types of patients with RP. Results also provide an indication that in RP the postreceptoral retinal pathways are not severely affected. The outcome of the present study is encouraging for future investigations with larger patient groups that are clinically more homogeneous and better characterized genetically.

Acknowledgments

The authors thank Galina Paramei for her constructive discussion of the results and her help with the manuscript.

Supported by grants from the German Research Council (DFG HU 2340/1-1 and KR 1317/16-1) as part of the Priority Program SPP2127.

Disclosure: C. Huchzermeyer, None; J. Fars, None; J. Kremers, None

References

- Swanson WH, Fish GE. Color matches in diseased eyes with good acuity: detection of deficits in cone optical density and in chromatic discrimination. *J Opt Soc Am A*. 1995;12:2230–2236.
- Jones BW, Marc RE. Retinal remodeling during retinal degeneration. *Exp Eye Res*. 2005;81:123–137, doi:10.1016/j.exer.2005.03.006.
- Strauss O. The retinal pigment epithelium in visual function. *Physiol Rev*. 2005;85:845–881, doi:10.1152/physrev.00021.2004.
- Donner KO, Rushton WaH. Retinal stimulation by light substitution. *J Physiol*. 1959;149:288–302.
- Estevez O, Spekrijse H. The “silent substitution” method in visual research. *Vision Res*. 1982;22:681–691.
- Shapiro AG, Pokorny J, Smith VC. Cone-rod receptor spaces with illustrations that use CRT phosphor and light-emitting-diode spectra. *J Opt Soc Am A*. 1996;13:2319–2328.
- Simunovic MP, Moore AT, MacLaren RE. Selective automated perimetry under photopic, mesopic, and scotopic conditions: detection mechanisms and testing strategies. *Transl Vis Sci Technol*. 2016;5, doi:10.1167/tvst.5.3.10
- Huchzermeyer C, Kremers J. Perifoveal S-cone and rod-driven temporal contrast sensitivities at different retinal illuminances. *J Opt Soc Am A*. 2017;34:171, doi:10.1364/JOSAA.34.000171.
- Huchzermeyer C, Martins CMG, Nagy B, et al. Photoreceptor-specific light adaptation of critical flicker frequency in trichromat and dichromat observers. *J Opt Soc Am A*. 2018;35:B106–B113, doi:10.1364/JOSAA.35.00B106.
- Cao D, Zele AJ, Pokorny J. Dark-adapted rod suppression of cone flicker detection: evaluation of receptor and postreceptor interactions. *Vis Neurosci*. 2006;23:531–537, doi:10.1017/S0952523806233376.
- Zele AJ, Cao D. Vision under mesopic and scotopic illumination. *Front Psychol*. 2014;5:1594, doi:10.3389/fpsyg.2014.01594.
- Zele AJ, Maynard ML, Joyce DS, Cao D. Effect of rod-cone interactions on mesopic visual performance mediated by chromatic and luminance pathways. *J Opt Soc Am A*. 2014;31:A7–A14.
- Zele AJ, Kremers J, Feigl B. Mesopic rod and S-cone interactions revealed by modulation thresholds. *J Opt Soc Am A*. 2012;29:A19–A26.
- Zele AJ, Cao D, Pokorny J. Rod-cone interactions and the temporal impulse response of the cone pathway. *Vision Res*. 2008;48:2593–2598, doi:10.1016/j.visres.2008.04.003.
- Cao D, Pokorny J, Smith VC. Matching rod percepts with cone stimuli. *Vision Res*. 2005;45:2119–2128, doi:10.1016/j.visres.2005.01.034.
- Cao D, Pokorny J, Smith VC, Zele AJ. Rod contributions to color perception: linear with rod contrast. *Vision Res*. 2008;48:2586–2592, doi:10.1016/j.visres.2008.05.001.
- Rabin J, Gooch J, Ivan D. Rapid quantification of color vision: the cone contrast test. *Invest Ophthalmol Vis Sci*. 2011;52:816–820, doi:10.1167/iovs.10-6283.
- Chacon A, Rabin J, Yu D, Johnston S, Bradshaw T. Quantification of color vision using a tablet display. *Aerosp Med Hum Perform*. 2015;86:56–58
- Smith VC, Pokorny J, Davis M, Yeh T. Mechanisms subserving temporal modulation sensitivity in silent-cone substitution. *J Opt Soc Am A*. 1995;12:241–249.
- Hardcastle AJ, Sieving PA, Sahel J-A, et al. Translational retinal research and therapies. *Transl Vis Sci Technol*. 2018;7:8, doi:10.1167/tvst.7.5.8.
- Roman AJ, Powers CA, Semenov EP, et al. Short-wavelength sensitive cone (S-cone) testing as an outcome measure for NR2E3 clinical treatment trials. *Int J Mol Sci*. 2019;20:2497, doi:10.3390/ijms20102497.
- McGuigan DB, Roman AJ, Cideciyan AV, et al. Automated light- and dark-adapted perimetry for evaluating retinitis pigmentosa: filling a need to accommodate multicenter clinical trials. *Invest Ophthalmol Vis Sci*. 2016;57:3118, doi:10.1167/iovs.16-19302.
- Graham N, Hood DC. Modeling the dynamics of light adaptation: the merging of two traditions. *Vision Res*. 1992;32:1373–1393.
- Pokorny J, Smithson H, Quinlan J. Photostimulator allowing independent control of rods and the three cone types. *Vis Neurosci*. 2004;21:263–267.

25. Huchzermeyer C, Kremers J. Perifoveal L- and M-cone-driven temporal contrast sensitivities at different retinal illuminances. *J Opt Soc Am A*. 2016;33:1989, doi:[10.1364/JOSAA.33.001989](https://doi.org/10.1364/JOSAA.33.001989).
26. Huchzermeyer C, Schlomberg J, Welge-Lüssen U, Berendschot TTJM, Pokorny J, Kremers J. Macular pigment optical density measured by heterochromatic modulation photometry. *PLoS One*. 2014;9:e110521, doi:[10.1371/journal.pone.0110521](https://doi.org/10.1371/journal.pone.0110521).
27. Neely DC, Bray KJ, Huisinigh CE, Clark ME, McGwin G, Owsley C. Prevalence of undiagnosed age-related macular degeneration in primary eye care. *JAMA Ophthalmol*. 2017;135:570–575, doi:[10.1001/jamaophthalmol.2017.0830](https://doi.org/10.1001/jamaophthalmol.2017.0830).
28. Ismail GM, Whitaker D. Early detection of changes in visual function in diabetes mellitus. *Ophthalmic Physiol Opt*. 1998;18:3–12.
29. Grover S, Fishman GA, Brown J. Patterns of visual field progression in patients with retinitis pigmentosa. *Ophthalmology*. 1998;105:1069–1075, doi:[10.1016/S0161-6420\(98\)96009-2](https://doi.org/10.1016/S0161-6420(98)96009-2).
30. Puts MJH, Pokorny J, Quinlan J, Glennie L. Audiophile hardware in vision science; the soundcard as a digital to analog converter. *J Neurosci Methods*. 2005;142:77–81, doi:[10.1016/j.jneumeth.2004.07.013](https://doi.org/10.1016/j.jneumeth.2004.07.013).
31. Stockman A, Sharpe LT, Fach C. The spectral sensitivity of the human short-wavelength sensitive cones derived from thresholds and color matches. *Vision Res*. 1999;39:2901–2927.
32. Stockman A, Sharpe LT. The spectral sensitivities of the middle- and long-wavelength-sensitive cones derived from measurements in observers of known genotype. *Vision Res*. 2000;40:1711–1737.
33. Wald G. Human vision and the spectrum. *Science*. 1945;101:653–658, doi:[10.1126/science.101.2635.653](https://doi.org/10.1126/science.101.2635.653).
34. Bates DM. lme4: mixed-effects modeling with R.:145.
35. Jang W, Lim J. PQL estimation biases in generalized linear mixed models. 15.
36. Werner JS, Steele VG. Sensitivity of human foveal color mechanisms throughout the life span. *J Opt Soc Am A*. 1988;5:2122–2130.
37. Knoblauch K, Vital-Durand F, Barbur JL. Variation of chromatic sensitivity across the life span. *Vision Res*. 2001;41:23–36.
38. Wuergler S, Xiao K, Fu C, Karatzas D. Colour-opponent mechanisms are not affected by age-related chromatic sensitivity changes. *Ophthalmic Physiol Opt*. 2010;30:653–659, doi:[10.1111/j.1475-1313.2010.00744.x](https://doi.org/10.1111/j.1475-1313.2010.00744.x).
39. Paramei GV, Oakley B. Variation of color discrimination across the life span. *J Opt Soc Am A*. 2014;31:A375, doi:[10.1364/JOSAA.31.00A375](https://doi.org/10.1364/JOSAA.31.00A375).
40. Ernst W, Clover G, Faulkner DJ. X-linked retinitis pigmentosa: reduced rod flicker sensitivity in heterozygous females. *Invest Ophthalmol Vis Sci*. 1981;20:812–816.
41. Tyler CW, Ernst W, Lyness AL. Photopic flicker sensitivity losses in simplex and multiplex retinitis pigmentosa. *Invest Ophthalmol Vis Sci*. 1984;25:1035–1042.
42. Dagnelie G, Massof RW. Foveal cone involvement in retinitis pigmentosa progression assessed through flash-on-flash parameters. *Invest Ophthalmol Vis Sci*. 1993;34:231–242.
43. Felius J, Swanson WH. Photopic temporal processing in retinitis pigmentosa. *Invest Ophthalmol Vis Sci*. 1999;40:2932–2944.
44. Pinckers A, van Aarem A, Keunen JE. Colour vision in retinitis pigmentosa. Influence of cystoid macular edema. *Int Ophthalmol*. 1993;17:143–146.
45. Lee SH, Yu HG, Seo JM, et al. Hereditary and clinical features of retinitis pigmentosa in Koreans. *J Korean Med Sci*. 2010;25:918–923, doi:[10.3346/jkms.2010.25.6.918](https://doi.org/10.3346/jkms.2010.25.6.918).
46. Kremers J, Scholl HP, Knau H, Berendschot TT, Usui T, Sharpe LT. L/M cone ratios in human trichromats assessed by psychophysics, electroretinography, and retinal densitometry. *J Opt Soc Am A*. 2000;17:517–526.
47. Sandberg MA, Berson EL. Blue and green cone mechanisms in retinitis pigmentosa. *Invest Ophthalmol Vis Sci*. 1977;16:149–157.
48. Greenstein VC, Hood DC, Ritch R, Steinberger D, Carr RE. S (blue) cone pathway vulnerability in retinitis pigmentosa, diabetes and glaucoma. *Invest Ophthalmol Vis Sci*. 1989;30:1732–1737.
49. Mollon JD. What is odd about the short-wavelength mechanism and why is it disproportionately vulnerable to acquired damage? *Doc Ophthalmol*. 33:145–149.
50. Hood DC, Benimoff NI, Greenstein VC. The response range of the blue-cone pathways: a source of vulnerability to disease. *Invest Ophthalmol Vis Sci*. 1984;25:864–867.
51. van der Veen RLP, Berendschot TTJM, Makridaki M, Hendrikse F, Carden D, Murray IJ. Correspondence between retinal reflectometry and a flicker-based technique in the measurement of macular pigment spatial profiles. *J Biomed Opt*. 2009;14:064046, doi:[10.1117/1.3275481](https://doi.org/10.1117/1.3275481).
52. Sun H, Pokorny J, Smith VC. Control of the modulation of human photoreceptors. *Color Res Appl*. 2001;26:S69–S75.